The Transoid, Ortho, and Gauche Conformers of Decamethyl-*n*-tetrasilane, *n*-Si_4Me_{10}: Electronic Transitions in the Multistate Complete Active Space Second-Order Perturbation Theory Description

Mari Carmen Piqueras and Raül Crespo*

Departament de Química Física i Institut de Ciència Molecular, Universitat de València, Dr. Moliner 50, E-46100 Burjassot (Valencia), Spain

Josef Michl*

Department of Chemistry and Biochemistry, University of Colorado, Boulder, Colorado 80309-0215

Received: December 30, 2002; In Final Form: March 11, 2003

Multistate complete active space second-order perturbation theory (MS-CASPT2) is used to improve earlier descriptions of the low-energy valence excited states of the transoid, ortho, and gauche conformers of decamethyl-*n*-tetrasilane, *n*-Si_4Me_{10}, using a generally contracted basis set of atomic natural orbitals (ANOs) at a ground-state geometry optimized in the second-order Møller−Plesset perturbation theory (MP2) approximation with Dunning's correlation consistent triple-ζ basis set (cc-pVTZ) on the silicon atoms and the 6-31G* and 6-31G basis sets on the carbon and hydrogen atoms, respectively. Relative energies, relative free energies, and mole fractions of the transoid, ortho, and gauche conformers are reported at various temperatures. CASPT2 ionization potentials for the three conformers are calculated and found to agree with photoelectron spectra. The first eight valence excited states of each conformer are computed and analyzed in terms of natural orbitals. Most of the important excitations are due to electron promotions from the σ_1 HOMO orbital. However, in the ortho and gauche conformers, promotions from the σ_2 HOMO-1 orbital play a significant and previously unrecognized role. The MS-CASPT2 simulation of the low-energy region of the absorption spectra of the transoid, ortho, and gauche conformers agrees with the UV absorption spectrum of the transoid conformer of *n*-Si_4Me_{10} and with the conformationally constrained models of the ortho and gauche tetrasilanes, $MeSi[(CH_2)_5]_2Si-Si[(CH_2)_5]_2SiMe$ and $(SiMe_2)_4(CH_2)_3$, respectively. The UV absorption spectra of *n*-Si_4Me_{10} conformer equilibrium mixtures at room temperature and 77 K are interpreted. An analysis of the dependence of the nature of electronic excitation on the skeletal dihedral angle confirms the main features of the previously developed picture, which described it in terms of avoided crossings of both B and A symmetry states. These cause the states to interchange their $\sigma\sigma^*$ and $\sigma\pi^*$ character upon going between the two planar limits, syn and anti. However, the new results show that at small dihedral angles the situation is more complicated because of additional avoided crossings.

Introduction

Polysilanes[1] have attracted considerable interest because of their remarkable optical and other properties, commonly attributed to σ electron delocalization. Peralkylation renders these fully saturated polymers very stable and potentially practically useful. Their most striking spectroscopic feature is the near-UV absorption, whose low excitation energy is qualitatively understandable as a consequence of the low electronegativity of silicon relative to the lateral substituents.[2] The great sensitivity of the absorption spectra of these materials to the detailed structure of the alkyl substituents, but also to factors such as temperature,[3] pressure,[4] and solvent,[5] is usually interpreted as due to the sensitivity of σ delocalization to backbone conformation.[1] The energy differences and barriers between the different conformations are typically quite small, and after years of effort, it is still not firmly established what most of these conformations are in the various spectroscopically characterized situations. In addition to its significance for the understanding of polysilanes, this would be of general interest for the theory of electron delocalization in interacting σ bonds.

In an effort to establish the nature of the possible backbone conformations[6,7] and their spectroscopic properties, much effort has also been invested in peralkylated oligosilanes containing up to about two dozen silicon atoms.[1] In these, computations suggest that three dihedral angles (∼55°, gauche; ∼90°, ortho; and ∼165°, transoid) are typically favored for rotation around each internal Si−Si bond in permethylated chains[8−11] and possibly up to five (also cisoid and deviant) in chains carrying longer alkyl groups.[12,13] In keeping with recently proposed nomenclature,[7] we reserve the term "anti" for a 180° dihedral angle and use the term "transoid" for angles near 165°.

The shortest permethylated oligosilane with an internal SiSi bond is decamethyl-*n*-tetrasilane, *n*-Si_4Me_{10}. In this species, the presence of a transoid and a gauche conformer is undisputed,[9,14] but the existence of the third predicted distinct conformer, ortho, has not been proven by unequivocal experiments. The authors of an electron diffraction study concluded that it was probable,[14] and it is further supported indirectly by the presence of the ortho dihedral angle in several cyclic and branched permethylated oligosilane chains.[15] Moreover, spectroscopic proofs for the

10.1021/jp022675p CCC: $25.00
Published on Web 05/17/2003

theoretically predicted presence of all three conformers in the closely related tetrasilane, Si_4Cl_{10}, by matrix isolation Raman spectroscopy[16] and in the more distantly related perfluorobutane, C_4F_{10}, by matrix isolation IR spectroscopy[17] have been provided. Thus, there is little reason to doubt the theoretically predicted existence of the gauche, ortho, and transoid conformers in *n*-Si_4Me_{10}.

Although so far it has not been possible to determine the electronic absorption spectra of all three conformers of *n*-Si_4Me_{10} separately, manipulation of UV and IR spectra recorded in annealed and/or irradiated low-temperature matrices permitted a separate determination of the UV and IR spectra of the transoid conformer (at the time called anti) and of an unknown linear combination of the UV spectra of the gauche and ortho conformers, which have essentially identical predicted IR spectra.[9] In addition, measurements on peralkylated tetrasilanes constrained to particular dihedral angles by saturated polymethylene chains provide a fair idea of the UV spectra of the peralkylated gauche tetrasilane, approximated by $(SiMe_2)_4(CH_2)_3$,[18] and ortho tetrasilane, approximated by $MeSi[(CH_2)_5]_2Si-Si[(CH_2)_5]_2SiMe$.[19] These suggest strongly that the approximate matrix isolation spectrum of the twisted form reported earlier[9] is dominated by the gauche conformer.

The spectra attributable to the three conformers do not support the original expectations, according to which the lowest energy singlet−singlet electronic transition in oligosilanes should always be of lower energy in the extended conformations than in the twisted ones. Indeed, for tetrasilanes the currently available evidence[18,19] shows clearly that it is not the energy but the intensity of the lowest transition that undergoes a pronounced change as the SiSiSiSi dihedral angle is varied. A theoretical interpretation of this observation was provided by low level (CIS/3-21G*) ab initio calculations for the peralkylated tetrasilanes;[9,18] similar results were obtained even earlier for the parent tetrasilane, Si_4H_{10}.[8,20,21] These results were in poor quantitative agreement with the experimental excitation energies but accounted qualitatively for the trends in the spectra of both the parent and the alkylated tetrasilanes as a function of the dihedral angle. They predicted the tetrasilane chromophore to have four low-lying valence states, two of A and two of B symmetry in the C_2 group. In the planar syn (C_{2v}) and anti (C_{2h}) conformation limits, one state of each symmetry is of the $\sigma\sigma^*$ type and the other of the $\sigma\pi^*$ type, and they change their energy order upon going from one limit to the other. Since a plane of symmetry is absent for all but the limiting dihedral angles, the expected state crossing is avoided, accounting for the observed approximate constancy of transition energies and the gradual transfer of intensity from the upper to the lower of the two transitions into states of B symmetry as the dihedral angle increases.

Recent calculations for the two conformers of the parent tetrasilane, Si_4H_{10}, performed at the MS-CASPT2 level, accounted quantitatively for the observed excitation energies. They were compatible with the avoided crossing notion outlined above but showed an even more complicated picture.[22,23] In the anti conformer, there are six valence excited states below the first Rydberg transition. They correspond to single-electron promotions from the highest occupied molecular orbital (HOMO) to four σ^* and two π^* valence orbitals. In the gauche conformer, there are eight valence excited states below the first Rydberg state. Here, lower symmetry precludes a strict classification of orbitals as σ or π, but closer inspection suggests that the distinction is still approximately valid and can be used for qualitative nomenclature purposes. Six of the states computed for the gauche conformer correlate with those of the anti conformer. The two additional states correspond to single-electron transitions from the σ_2 HOMO-1 to the σ_1^* and σ_2^* valence orbitals. Excitations from the σ_2 orbital had not been emphasized previously.

It appeared very desirable to obtain a quantitative description of the excited states of the three conformers of *n*-Si_4Me_{10} at a level similar to that now available for the two conformers of the parent Si_4H_{10}, and to find out whether the general description of trends deduced from very approximate theories stands up to close scrutiny or needs to be modified. The results thus could serve as a benchmark for evaluating approximate procedures suitable for calculations on longer oligosilanes. Presently, we report and discuss the results of multiconfigurational second-order perturbation theory (MS-CASPT2) calculations for the low-lying excited states for the gauche, ortho, and transoid conformers of *n*-Si_4Me_{10}.

Computational Methods

All calculations have been performed at the equilibrium geometries of the ground state of the transoid, ortho, and gauche conformers of *n*-Si_4Me_{10}, obtained using the second-order Møller−Plesset perturbation theory (MP2) as implemented in the Gaussian-98 suite of programs.[24] The geometry optimizations employed Dunning's correlation consistent triple-ζ basis set (cc-pVTZ)[25] for the silicon atoms and the 6-31G* and 6-31G basis sets for the carbon and the hydrogen atoms, respectively. The MP2(fc) geometry optimization calculations were carried out within the C_2 symmetry point group constraints, with *z* as the twofold symmetry axis. Relative free energies have been calculated in the harmonic approximation by adding rotational entropy and vibrational entropy contributions calculated at the HF/6-31G* level and scaled[26] by 0.9135.

Electronic properties were computed from complete active self-consistent field (CASSCF) wave functions employing a generally contracted basis set of atomic natural orbitals (ANOs) obtained from Si(17s12p5d4f)/C(14s9p4d3f)/H(8s4p) primitive sets[27] using the Si[5s4p1d]/C[3s2p1d]/H[2s] contraction scheme. The reference wave function and the molecular orbitals were obtained from average CASSCF calculations, where the averaging included the four A and four B symmetry states of interest. All four 1s core orbitals of the silicon atoms were kept frozen, as determined by the ground-state SCF wave function. The active space used in all calculations was (5,4), where the numbers specify the number of active orbitals belonging to the a and b irreducible representations of the C_2 point group, respectively. The active space has been chosen to include the six σ and σ^* Si−Si bond orbitals, plus one σ^* and two π^* Si−Me bond orbitals. The selection of the active space was made on the basis of our previous CASPT2 studies of the electronic spectra of trisilane[28] and *n*-tetrasilane.[22,23] In all calculations the number of active electrons was set to six, which corresponds to the three Si−Si bonds of the σ-conjugated system of the molecule. Although the symbols σ and π are not strictly applicable to a molecule without a plane of symmetry, they are applicable qualitatively, and for easy comparison, we have labeled the NOs of all conformers accordingly. The symbol σ is used for orbitals composed primarily of backbone sp^3 hybrids on silicon, and the symbol π for those composed mostly of out-of-phase combinations of its lateral sp^3 hybrids.

Single-state second-order perturbation theory with a multiconfigurational reference state, the CASPT2 approach,[29] was used to account for the remaining dynamical correlation effects. The CASPT2 method calculates the first-order wave function

TABLE 1: MP2(fc)/cc-pVTZ/6-31G*/6-31G Optimized Ground-State Geometry, Relative Energy, Relative Free Energy, and Mole Fraction of Gauche, Ortho, and Transoid Conformers of *n*-Si_4Me_{10}

property[a]	MP2			exp[b]		
	gauche	ortho	transoid	gauche	ortho	transoid
$r_{Si(1)Si(2)}$	2.354	2.354	2.354	2.351(6)	2.345(6)	2.350(6)
$r_{Si(2)Si(3)}$	2.353	2.358	2.353	2.354(6)	2.359(6)	2.354(6)
$r_{Si(1)C}$	1.888, 1.889, 1.891	1.887, 1.889, 1.891	1.889, 1889, 1.890	1.893(2)	1.893(2)	1.893(2)
$r_{Si(2)C}$	1.899, 1.902	1.899, 1.901	1.899, 1.899	1.903(2)	1.903(2)	1.901(2)
r_{CH}	1.094−1.096	1.095−1.096	1.095−1.096	1.094(2)	1.095(2)	1.094(2)
∠Si(1)Si(2)Si(3)	114.1	112.4	110.2	117.0(5)	115.1(5)	112.4(5)
∠Si(1)Si(2)Si(3)Si(4)	54.5	91.3	162.6	[55][c]	[92][c]	163(8)
ΔE[d]	0.27 (0.31)[e]	0.67 (0.74)[e]	0.0			
ΔG^{77} [d]	0.36	0.73	0.0			
ΔG^{298} [d]	0.59	0.79	0.0			
ΔG^{340} [d]	0.63	0.81	0.0			
χ_{77}[f]	0.08	0.01	0.91			
χ_{298} [f]	0.23	0.16	0.61			
χ_{340} [f]	0.23	0.18	0.59	0.31(8)	0.17(14)	0.51(6)

[a] Distances in angstroms and angles in degrees. [b] Values from ref 14. [c] Values from B3PW91/6-311G* calculations. [d] Values of relative potential energies (ΔE) and relative free energies (ΔG) in kilocalories per mole. [e] Scaled zero-point energies included. [f] Values of mole fraction (χ) computed from free energies.

and the second-order energy, with a CASSCF[30] wave function constituting the reference function. Orbitals and transition energies are obtained at this level. The coupling of the CASSCF wave functions via dynamic correlation was evaluated using the extended multistate CASPT2 (MS-CASPT2) method.[31] The MS-CASPT2 method gave good results for trisilane[28] and *n*-tetrasilane,[22,23] where average CASSCF calculations introduce a strong mixing of Rydberg and valence states. Additional intruder states weakly interacting with the reference CASSCF wave function were handled by the level shift technique.[32] A level shift of 0.05 has been used in all calculations to remove all intruder-state problems without affecting the excitation energies (<0.1 eV).

Transition dipole moments were computed with the CASSCF state interaction (CASSI) method[33] and combined with MS-CASPT2 energy differences to obtain oscillator strengths. To compute MS-CASPT2 oscillator strengths, the perturbation modified CAS (PMCAS) reference functions[31] obtained as linear combinations of all CAS states involved in the MS-CASPT2 calculation were used. These methods and techniques are well-established approaches to the study of electronic excitation spectra of oligosilanes.[22,23,28] The MS-CASPT2 calculations have been performed with the MOLCAS-5 quantum chemistry software.[34]

Results

Conformer Geometries. Representative features of the MP2/cc-pVTZ/6-31G*/6-31G optimized geometries of the isolated molecules of the transoid, ortho, and gauche conformers of *n*-Si_4Me_{10} are given in Table 1 together with the available experimental data.[14] These geometries were used in all computations described below.

All levels of calculation, starting with the simplest models[6] to MM2 and MM3 empirical force field methods,[10] the B3LYP/6-31G(d) and B3LYP/3-21G(d) DFT methods,[11] and the HF/3-21G*,[8] MP2/3-21G*,[9] MP2/6-31G*,[9] and, now, MP2/cc-pVTZ/6-31G*/6-31G ab initio methods, show the existence of three distinct potential energy minima that correspond to the gauche, ortho, and transoid conformers. The presently calculated dihedral angles of 54.5°, 91.3°, and 162.6°, respectively, presumably represent the most reliable values available to date.

Conformer Energies and Abundancies. All methods of calculation agree that the transoid conformer is the most stable. Previous MP2/6-31G*//HF/3-21G* calculations,[10] including vibrational zero point energies, suggested that, for an isolated molecule, the relative energy of the gauche conformer is 0.24 kcal/mol and that of the ortho is 0.65 kcal/mol higher. The present results (Table 1), 0.31 and 0.74 kcal/mol, respectively, are quite close. Relative free energies were used to compute mole fractions at three different temperatures and have been included in Table 1.

TABLE 2: CASPT2 Ionization Potentials (eV) of Transoid, Ortho, and Gauche Conformers of *n*-Si_4Me_{10} and Observed Photoelectron Spectra of *n*-Si_4Me_{10}

compd	1^2A	1^2B	2^2A
conformer			
transoid[a]	7.58	8.68	8.78
ortho[a]	7.72	8.33	8.93
gauche[a]	7.79	8.19	9.07
mixture[b]			
ref 35	7.98	8.76	9.30
ref 36	∼8.0	∼9.0	∼9.2

[a] Calculated. [b] Peak energy.

Photoelectron Spectra. The vertical ionization potentials of the three conformers of *n*-Si_4Me_{10} calculated at the CASPT2 level and those derived from He(I) photoelectron spectra of the conformer mixture[35,36] are collected in Table 2.

Electronic Transitions. The vertical excitation energies and oscillator strengths of the singlet valence states of the transoid, ortho, and gauche conformers of *n*-Si_4Me_{10} calculated at the MS-CASPT2 level are listed in Table 3. The values for the first ionization potential of the three conformers of *n*-Si_4Me_{10} lie near 7.5 eV, and we therefore list only states with excitation energies up to 6.5 eV. All of these are valence states. The electronic transitions are dipole-allowed and are located in three well-defined energy intervals near 5.3, 6.0, and 6.5 eV. All low-energy transitions with significant intensity are polarized approximately along the Si1−Si4 line. Several of the higher energy states have not been reported previously.

In terms of natural orbitals (NOs), the description of the wave functions of the four lowest energy excited states becomes quite simple. These excitations can be described as single electron promotions from an NO that is nearly doubly occupied in the ground state to one that is nearly empty in the ground state, as the excited state density matrix is characterized by two NOs whose occupancy is very close to unity. The NOs deduced from the density matrices of any one of these states are virtually indistinguishable, and the two NOs from which electron

TABLE 3: MS-CASPT2 Vertical Excitation Energies (*E*, eV), Oscillator Strengths (*f*), and Transition Moment Directions (α[a]) in Transoid, Ortho, and Gauche Conformers of *n*-Si_4Me_{10}

transoid				ortho				gauche			
state	*E*	*f*	α	state	*E*	*f*	α	state	*E*	*f*	α
1^1B ($\sigma_1\sigma_1^*$)	5.28	0.585	26	2^1A ($\sigma_1\sigma_2^*$)	5.34	0.053		2^1A ($\sigma_1\sigma_2^*$)	5.42	0.115	
2^1A ($\sigma_1\pi_1^*$)	5.38	0.001		1^1B ($\sigma_1\sigma_1^*$)	5.38	0.326	18	1^1B ($\sigma_1\sigma_1^*$)	5.53	0.069	13
3^1A ($\sigma_1\sigma_2^*$)	5.87	0.0001		3^1A ($\sigma_1\pi_1^*$)	5.93	0.004		2^1B ($\sigma_2\sigma_2^*$)	5.91	0.316	16
2^1B ($\sigma_1\pi_2^*$)	5.99	0.027	65	2^1B ($\sigma_2\sigma_2^*$)	5.94	0.215	10	3^1A ($\sigma_2\sigma_1^*$)	5.96	0.015	
4^1A	6.46	0.036		4^1A	6.11	0.043		4^1A	6.10	0.001	
3^1B	6.46	0.007	26	3^1B	6.29	0.015	32	3^1B	6.34	0.001	−27
4^1B	6.51	0.221	66	4^1B	6.58	0.119	43	4^1B	6.55	0.120	16
5^1A	6.54	0.247		5^1A	6.68	0.015		5^1A	6.64	0.039	

[a] Transitions into A states are polarized along the *z* axis. Directions of transitions into B states lie in the *xy* plane and form an angle α with the Si(2)Si(3) bond, taken positive if the moment is inclined toward the projection of the Si(1)Si(4) line.

promotions take place also are visually indistinguishable from the two highest occupied Hartree−Fock orbitals. All the NOs are valence orbitals, and their nodal properties are those expected from Hückel considerations. This correspondence is used for orbital labeling, which is based on the number of nodal surfaces. In the transoid conformer, this corresponds exactly to the energy order of the excited states, too. For the higher energy states, the picture becomes more complicated in that some of them are intrinsically multiconfigurational and their NO occupation numbers have significantly nonintegral values. We do not attempt to describe the nature of these states here in detail.

The first electronic transitions are nearly degenerate in all three conformers. One is into the 1^1B state. In the transoid conformer, it occurs at 5.28 eV and is the most strongly allowed, with an oscillator strength of ∼0.6. The energy of this state increases upon going to the ortho (5.38 eV) and to the gauche (5.53 eV) conformers, and the oscillator strength drops to ∼0.3 and ∼0.07, respectively. This is an electronic transition from the σ_1 HOMO to the σ_1* LUMO orbital and is the one that is normally considered the most characteristic of oligosilanes. The other transition, nearly isoenergetic, is from the ground state to the 2^1A excited state. It has similar calculated energies in all three conformers, ∼5.4 eV. The oscillator strength is essentially negligible for the transoid conformer and increases up to ∼0.1 for the gauche conformer. This electronic transition corresponds to the excitation from the σ_1 HOMO into the π_1* orbital in the transoid conformer, but from the σ_1 HOMO into the σ_2* orbital in the ortho and gauche conformers. The third excited state (3^1A) lies very close to the fourth (2^1B) in all conformers and carries negligible oscillator strength. It corresponds to a one-electron promotion from the σ_1 HOMO to the σ_2* orbital in the transoid conformer, from the σ_1 HOMO to the π_1* orbital in the ortho conformer, and from the σ_2 HOMO-1 to the σ_1* orbital in the gauche conformer. In the transoid conformer, the 2^1B excited state corresponds mostly to a one-electron promotion from the σ_1 HOMO to the π_2* orbital, with a small contribution from the promotion of an electron from the σ_2 HOMO-1 to the σ_2* orbital. In the ortho and gauche conformers, it is described approximately by the promotion of an electron from the σ_2 to the σ_2* orbital, with a small contribution from the σ_1 to π_2* excitation. The oscillator strength of this electronic transition increases strongly from the transoid (∼0.03) to the ortho (∼0.2) and the gauche (∼0.3) conformers. The remaining electronic transitions, to the 3^1B and 4^1A excited states, located very close in energy, and to the 4^1B and 5^1A states, again computed at almost the same energy, are mostly of multiconfigurational character.

In the following, we compare the best experimental information available for the UV absorption spectra of the individual conformers with the MS-CASPT2 simulation assuming the spectral line shapes to be Gaussian functions with a full width at half-maximum of 0.3 eV, as in previous studies.[22,23,28] Solvent effects have been neglected.

Transoid Conformer. The UV absorption spectrum of this conformer was extracted[9] from the spectra of various conformer mixtures recorded in an Ar matrix at 12 K. It is displayed in Figure 2 together with a MS-CASPT2 simulation.

The first spectral interval is dominated by a strong band mainly due to an electronic transition to the 1^1B state located at 5.28 eV. Its oscillator strength (∼0.6) is the highest of all among the electronic transitions calculated for the three conformers of *n*-Si_4Me_{10}. This first band is also calculated to contain a minor contribution from a very weak transition to the 2^1A valence state, computed to lie at 5.38 eV.

The second spectral interval has almost no calculated or observed intensity. The calculated transition into a 2^1B (5.99 eV) state is weak, and that into the 3^1A (5.87 eV) state is even weaker.

The third spectral interval, near 6.5 eV, contains rising end absorption, assigned to the superposition of two strong electronic transitions to the 4^1B and 5^1A valence states, computed at 6.51 and 6.54 eV. The transition into the 5^1A state and, to a smaller degree, also the one into the 4^1B state are the only ones that show a large short-axis polarized intensity, and this might be detectable in linear dichroism. There are also some minor contributions to this band from weak transitions into the 3^1B and 4^1A valence states.

Ortho Conformer. The analysis of matrix isolation spectra that yielded the spectrum of the pure transoid conformer only produced a spectrum of an unknown mixture of the ortho and gauche conformers.[9] In view of the calculated composition of the conformer equilibrium at room temperature, this must be dominated by the spectrum of the gauche form. The best that we can do at present to approximate the absorption spectrum of the ortho conformer is to use the one reported[19] for a room-temperature solution of a conformationally constrained tetrasilane, $MeSi[(CH_2)_5]_2Si-Si[(CH_2)_5]_2SiMe$.

Unlike the spectra of the other two conformers, the spectrum of the ortho conformer (Figure 3) shows a strong absorption peak in each of the three spectral regions. The first two are well developed at 5.5 and 6.1 eV, respectively, and there is an indication of the third one near 6.5 eV.

In the first region, in addition to the prominent absorption peak at 5.5 eV, attributed to a transition to the 1^1B state (calculated at 5.38 eV), linear dichroism revealed a differently polarized additional weak transition near 5.1 eV. This is calculated at 5.34 eV (2^1A excited state).

In the second spectral region, the calculations predict four transitions, only one of which is strong. It lies at 5.94 eV (2^1B) and has an oscillator strength of ∼0.2. One of the additional

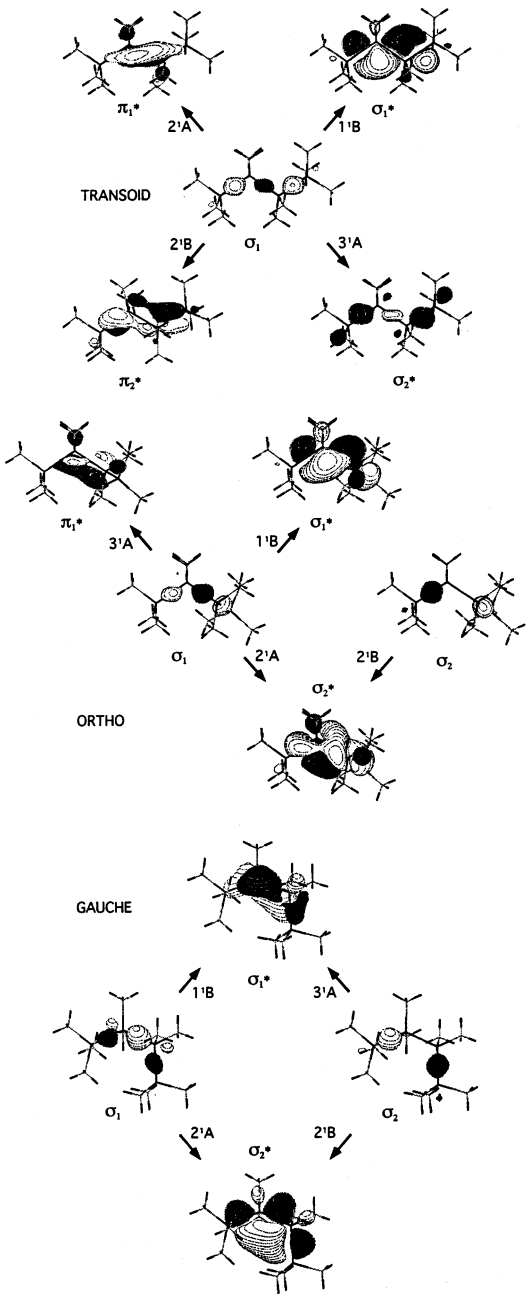

Figure 1. Natural orbitals with occupation numbers close to unity obtained from the perturbation-modified CAS (PMCAS) wave functions of the valence excited states of *n*-Si_4Me_{10} (the isodensity surface values are 0.018, except for π_2* and σ_2* in the transoid conformer, for which the value is 0.007).

weak transitions also is of B symmetry, at 6.29 eV (3^1B), and two are of A symmetry, at 5.93 eV (3^1A) and a somewhat stronger one at 6.11 eV (4^1A).

The third spectral region contains a strong transition at 6.58 eV into the 4^1B state and a weak one at 6.68 eV into the 5^1A state.

Gauche Conformer. The analysis of matrix isolation spectra of conformer mixtures that yielded the spectrum of the pure transoid conformer also produced a more approximate tentative spectrum of an unknown mixture of the ortho and gauche conformers,[9] undoubtedly dominated by the spectrum of the gauche form. In addition to this spectrum, Figure 4 shows the matrix isolation UV spectrum of a conformationally constrained cyclic tetrasilane $(SiMe_2)_4(CH_2)_3$, characterized by a gauche

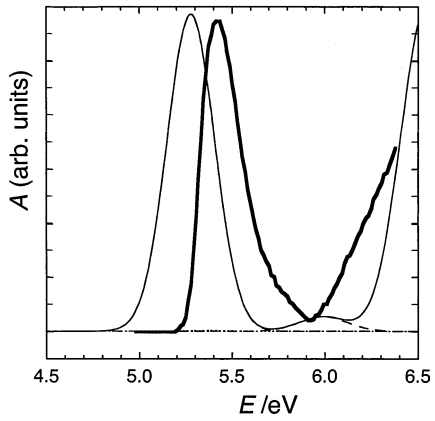

Figure 2. Transoid conformer of *n*-Si_4Me_{10}: The UV absorption spectrum deduced from experiment[9] (thick solid line), and MS-CASPT2 simulation of the low-energy region assuming a 0.3 eV full width at half-maximum (—), with individual contributing Gaussians shown (transitions into A, · · ·, and B, - - -, states).

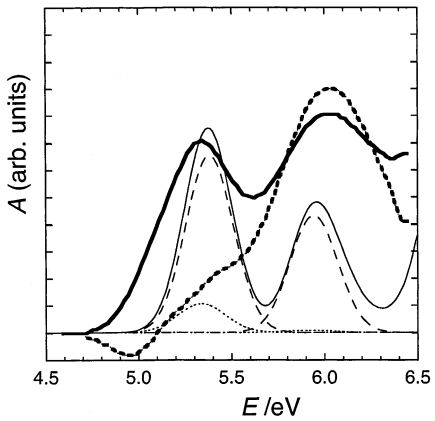

Figure 3. Ortho conformer of *n*-Si_4Me_{10}: The observed UV (thick solid line) and LD (thick dashed line) spectra of the conformationally constrained ortho tetrasilane, $MeSi[(CH_2)_5]_2Si-Si[(CH_2)_5]_2SiMe$,[19] and MS-CASPT2 simulation of the low-energy region assuming a 0.3 eV full width at half-maximum (—), with individual contributing Gaussians shown (transitions into A, · · ·, and B, - - -, states).

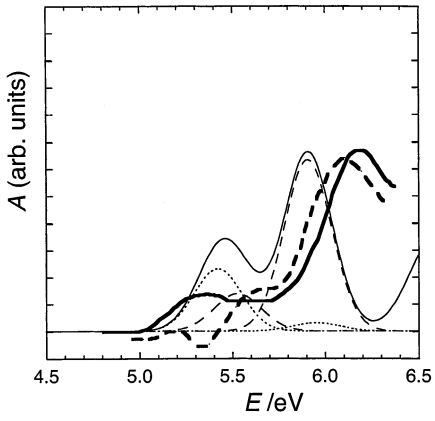

Figure 4. Gauche conformer of *n*-Si_4Me_{10}: The UV absorption spectrum deduced from experiment[9] (thick dashed line), the spectrum of the conformationally constrained gauche tetrasilane, $(SiMe_2)_4(CH_2)_3$[18] (thick solid line), and MS-CASPT2 simulation of the low-energy region assuming a 0.3 eV full width at half-maximum (—), with individual contributing Gaussians shown (transitions into A, · · ·, and B, - - -, states).

dihedral angle,[18] which probably is a better quality representation of the UV absorption of gauche *n*-Si_4Me_{10}.

The first spectral region contains a peak of moderate intensity located at 5.3 eV and an indistinct band of similar

intensity near 5.6 eV. The latter is much more clearly apparent in the MCD spectrum[37] and also in tetrasilanes with a smaller dihedral angle,[18] and there is no doubt about its existence even though it is hard to distinguish from the first band in Figure 4. Their symmetries have not been established experimentally. The band at 5.3 eV is presently attributed to a transition to the 2^1A state computed at 5.42 eV, and the band near 5.6 eV is assigned to the 1^1B state. However, since the cyclic tetrasilane $(SiMe_2)_4(CH_2)_3$ is only a model for gauche *n*-Si_4Me_{10}, and since the computed energy difference of the two states is small, we cannot tell the order of the observed states with certainty.

The second spectral region contains a much more intense band at 6.2 eV. According to the MS-CASPT2 calculations, it is due to the superposition of a strongly allowed transition into the 2^1B state at 5.91 eV and weak transitions into the 3^1A state at 5.96 eV and the 4^1A state at 6.10 eV.

The third spectral region lies at the edge of the experimental spectrum and contains an intense transition calculated to occur at 6.55 eV into the 4^1B state, a weak one at 6.64 eV into the 5^1A state, and a very weak one at 6.34 eV into the 3^1B state.

Discussion

Geometries. The computed and observed values are in very good accord. In the case of SiSi bond lengths, the agreement is significantly better than that obtained at the DFT level (B3PW91/6-311G*).[14] The values of dihedral angles are probably also more correct, but a comparison is difficult, since in the analysis of the electron diffraction data these were not optimized but assumed equal to the B3PW91/6-311G* values. For the gauche and ortho conformers, these DFT calculations were not converged to actual potential energy minima, and the values listed were only interpolated. In another DFT study[11] of the geometries of the three conformers, using the B3LYP/6-31G(d) and B3LYP/3-21G(d) methods, all three minima were located, but their geometries were found to be in only fair agreement with MP2/3-21G*[10] results. It was suggested that, in this case, DFT methods are inferior, presumably because a correct description of nonbonded interactions between substituents is essential, and the currently available functionals do not describe van der Waals attractions well. However, the MP2/3-21G* geometry optimization[10] gave SiSi bond lengths that were too short, and in this regard HF/3-21G* results[9] were better. The good agreement between calculated and experimental values obtained in this and previous[22,23,28] studies validates the use of MP2/cc-pVTZ/6-31G*/6-31G optimized geometries to treat peralkylated oligosilanes.

Conformer Energies and Abundancies. The mole fractions of the three conformers at the 67 °C temperature of the electron diffraction experiment, calculated from free energies, agree well with those deduced from this gas-phase experiment.[14] The free energies calculated for the ortho and gauche conformers are a little lower than those found earlier.[10] As a consequence, the mole fraction of the transoid conformer is lower than that reported previously.[10] In solution, the transoid conformer has been reported to be about 0.5 kcal/mol more stable than the twisted conformer, on the basis of temperature-dependent IR and Raman measurements and assuming that there is only one of the latter.[38] In inert-gas low-temperature matrixes, the transoid form is clearly the most stable.[9]

The HF[8] and DFT[11,14] methods underestimate the energy difference between the minor conformers relative to the MP2 method. Thus, the relative energies (in kcal/mol, without ZPE corrections) obtained for the gauche and ortho conformers, respectively, are 0.70 and 0.89 (HF/3-21G*[8]), 0.45 and 0.50 (B3LYP/6-31G(d)[11]), 0.68 and 0.71 (B3PW91/6-311G*[14]), but 0.09 and 0.65 (MP2/6-31G*[9]) and 0.27 and 0.67 (MP2/cc-pVTZ/6-31G*/6-31G).

Photoelectron Spectra. The values of the first and third ionization potentials calculated in this study are a little lower than those observed experimentally for a mixture of conformers, and the values calculated for the second ionization potentials agree the best. As expected, the ionization potentials of the three conformers are similar but not identical and the trends agree with those found for a series of tetrasilanes with constrained dihedral angles by experiment and previous calculations using Koopmans' theorem at the HF/TZ[39] and HF/3-21G*[36] levels, but the predicted difference between the first and second ionization potentials is now significantly smaller. The first ionization potentials of the three conformers (1^2A) differ by only 0.21 eV. The second ionization potential is highest in the transoid conformer and decreases appreciably when passing to the ortho and gauche conformers. This reduces the difference between the first two potentials from 1.10 to 0.61 and 0.40 eV as the dihedral angle decreases. The values computed for the third ionization potential also increase as the dihedral angle decreases. As a consequence, the difference between the second and the third ionization potentials increases appreciably as the dihedral angle decreases (0.10 eV for the transoid, 0.60 eV for the ortho, and 0.88 eV for the gauche conformer). The trends are understandable in terms of simple MO arguments.[39]

UV Spectra. The agreement between observed and calculated spectra for each of the three conformers is excellent, and the differences between them are rendered correctly. Thus, it is not a surprise that the spectrum of the mixture is reproduced well, too. This confirms our earlier conclusion[22,23,28] regarding the ability of the present procedure to calculate correctly the low-energy valence states of oligosilanes without explicit consideration of Rydberg orbitals.

The present results provide useful guidance for the continuing experimental search for additional low-energy transitions. So far, only three of the numerous predicted valence transitions of the tetrasilane chromophore have been individually observed, two into B states and one into an A state,[18,19,37] and one might hope that at least the fourth transition calculated in the first spectral region, which would be the second into an A state, would be amenable to detection despite its predicted weakness. Also, the transitions predicted at higher energies could be identifiable. For instance, the transition into the 5A state of the transoid conformer is short-axis polarized and might be detectable in linear dichroism. Similarly, in the second spectral region of the ortho conformer, the calculations predict four transitions, only one of which is strong and has been observed.

It is interesting to consider the striking spectral changes predicted as a function of the dihedral angle. With only three conformers, we do not quite have enough points to draw a correlation diagram. At first sight, the simple general picture of avoided crossings of two B states and two A states derived from more approximate methods[8,9,18,20,21] appears to remain valid, although we recognize the potential complications due to the presence of additional states, as suggested by the MS-CASPT2 results[23] for the parent *n*-tetrasilane.

In the simple picture a strongly allowed $\sigma_1\sigma_1^*$ configuration of B symmetry is low in energy at large dihedral angles and high in energy at small dihedral angles, for reasons obvious already at the Hückel level description using the simple ladder C model.[40,41] As the dihedral angle varies, this $\sigma\sigma^*$ configuration exchanges positions with a weakly allowed $\sigma\pi^*$ configuration, also of B symmetry. Since a plane of symmetry is absent at

intermediate values of the dihedral angle, $\sigma\sigma^*$ and $\sigma\pi^*$ configurations mix, and an avoided crossing results. In agreement with this description, the calculated excitation energy of the 1^1B state hardly changes at all as the dihedral angle decreases, but the oscillator strength it carries drops steeply as the state evolves from predominantly $\sigma\sigma^*$ to predominantly $\sigma\pi^*$ in nature, and is already negligible at the gauche conformer geometry. The excitation energy of the 2^1B state is also nearly constant for the three conformers, while the associated oscillator strength increases significantly as the dihedral angle decreases and the state evolves from $\sigma\pi^*$ to $\sigma\sigma^*$, and is quite large in the gauche conformer. These trends agree with experimental observations. The avoided crossing of weakly allowed $\sigma\sigma^*$ and $\sigma\pi^*$ states of A symmetry is less obvious in the results given in Table 3. The 2^1A state displays a behavior opposite to that of the 1^1B state, and its computed oscillator strength grows as the dihedral angle decreases, again in agreement with observations. However, so does the even smaller oscillator strength predicted for the so far unobserved 3^1A state.

Although it would thus initially appear that the present results fully support this simplest picture of the excited states as a function of the dihedral angle, they suggest (Table 3) that the B states undergo another avoided crossing at small dihedral angles, with a configuration involving electron promotion from the σ_2 HOMO-1 orbital. This complicates the situation by changing the nature of the wave function assigned to the second observed state of B symmetry, relative to the previous description. The important role of excitations from the σ_2 HOMO-1 orbital at small dihedral angles has already been noted in *n*-Si_4H_{10}.[23] To provide definitive answers, however, it will be necessary to perform calculations of the present quality for a larger number of dihedral angles and to establish the configuration and state correlation diagrams reliably.

Absorption Spectrum of *n*-Si_4Me_{10}. Using the computed conformer populations, it is now possible to use the MS-CASPT2 results to account for the ordinary absorption spectra of *n*-Si_4Me_{10} equilibrium conformer mixtures under room- and low-temperature conditions, as shown in Figure 5. The interpretation of the room-temperature spectrum is quite complex. The first band is due to six electronic transitions, two from each conformer. The main contribution to the band is the quite strongly allowed excitation of the transoid conformer to its 1^1B valence state located at 5.28 eV. The second strongest contribution, about seven times weaker, is due to the 1^1B state of the ortho conformer that lies at 5.38 eV, even though this is present in only a small amount in the room-temperature mixture. At this same energy is located the 2^1A state of the transoid conformer, which has a negligible effect on the spectrum, as it has an almost zero oscillator strength. The other three contributions to the band are from the 2^1A state of the ortho conformer, located at 5.34 eV, and from the 2^1A and 1^1B states of the gauche conformer, computed at 5.42 and 5.53 eV, respectively. These three electronic transitions have very similar oscillator strengths, several times smaller than that carried by the 1^1B state of the ortho conformer. The smaller fractions of the ortho and gauche conformers in the mixture (16 and 23%, respectively), together with this low oscillator strength, make their influence on the observed spectrum quite small.

The onset of the second UV absorption band is also due to the superposition of six electronic transitions, two from each conformer. Now, there are only three main contributions. One of them is the strongly allowed excitation into the 2^1B valence state of the gauche conformer located at 5.91 eV. Another originates from the excitation of the ortho conformer to its 2^1B valence state located at 5.94 eV, and is about half of that of the gauche conformer. The third significant contribution to the band is provided by the 2^1B state of the transoid conformer with an effect that is half of that of the ortho conformer. The other three contributions to the band are from the 3^1A states of the three conformers, computed at 5.87, 5.93, and 5.96 eV, respectively. These electronic transitions have very small oscillator strengths. The higher energy region of the second band is due to the superposition of 12 electronic transitions, four from each conformer. The main contributions are due to the 4^1B and 5^1A states of the transoid conformer, which have quite large oscillator strengths. There are also smaller contributions, about a sixth each, from the 4^1A state of the transoid conformer and from the 4^1B state of the ortho and gauche conformers.

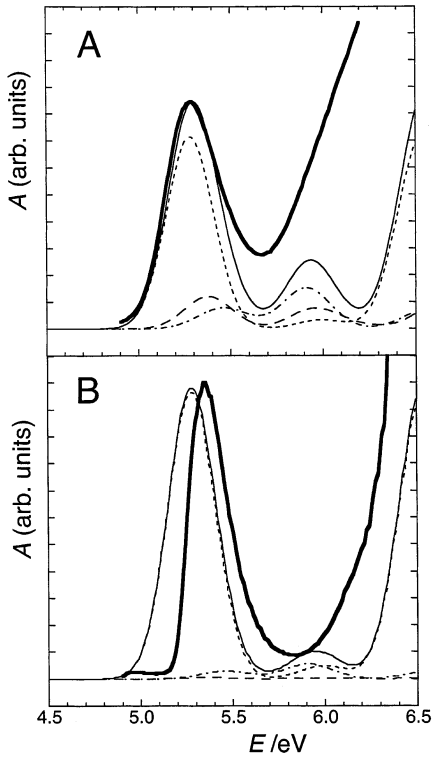

Figure 5. UV absorption spectra of the equilibrium conformer mixture of *n*-Si_4Me_{10} at room temperature (A) and 77 K (B): MS-CASPT2 simulations of the low-energy region assuming a 0.3 eV full width at half-maximum (—), and observed spectra (thick solid line). Individual computed contributions from the transoid (- - -,), ortho (— · —), and gauche (— — —) conformers are indicated.

In summary, the lower energy band in the room-temperature spectrum is mainly due to the 1^1B state of the transoid conformer, with small contributions from the ortho and gauche conformers. The low-energy region of the next observed band is mainly due to excitation of the gauche conformer with a significant contribution from the ortho conformer and a smaller contribution from the transoid conformer. The higher energy region is mainly due to excitation of the transoid conformer with small contributions from the ortho and gauche conformers.

The interpretation of the 77 K spectrum is less complex, as only the transoid conformer is present in significant amounts in the mixture and dominates the spectrum (91, 1, and 8% of the transoid, ortho, and gauche conformers, respectively). The first band is due to the strongly allowed excitations of the transoid conformer to its 1^1B valence state located at 5.28 eV. The other five contributions to the band from the 1^1B states of the ortho and gauche conformers and the 2^1A states of the three conformers have almost no effect on the shape of the band

except for the 1^1B state of the ortho conformer, whose contribution is about a sixteenth of the main one.

The lower part of the second energy band is due to the superposition of the electronic transitions from the 2^1B states of the three conformers, which make quite similar contributions to the band. Another weak contribution to the band comes from the 3^1A states of the three conformers and totals about a tenth of the overall contribution from the 2^1B states. The high-energy part of this band is mainly due to electronic transitions in the transoid conformer, primarily to its strongly allowed 4^1B and 5^1A states. There is also a small contribution from the 4^1A state of the transoid conformer and the 4^1B state of the gauche conformer.

Conclusions

The MS-CASPT2 method provides a very satisfactory description of the first eight valence excited states of the three conformers of *n*-Si_4Me_{10}, transoid, ortho, and gauche, and accounts for their individual UV absorption spectra, as well as the spectra of their equilibrium mixtures as a function of temperature. The results confirm the gross features of the previously developed description of the dependence of the UV absorption spectrum of the tetrasilane chromophore on the skeletal dihedral angle in terms of avoided crossings of both B and A symmetry states, which cause them to interchange their $\sigma\sigma^*$ and $\sigma\pi^*$ character upon going between the two planar limits, syn and anti. However, it suggests that at small dihedral angles the situation is more complicated because of additional avoided crossings. A full elucidation of the angular dependence will require computations for a larger number of dihedral angles and construction of the correlation diagram.

Acknowledgment. This work was supported by MCYT and European Feder Funds (Project BQU2001-2935-C02-01), the European Commission IST-2001-32243 contract, and the U.S. National Science Foundation (Grant CHE-0140478). J.M. is grateful to the University of Valencia for supporting a stay in Valencia.

References and Notes

(1) Miller, R. D.; Michl, J. *Chem. Rev.* **1989**, *89*, 1359. Michl, J.; West, R. In *Silicon-Containing Polymers: The Science and Technology of their Synthesis and Applications*; Jones, R. G., Ando, W., Chojnowski, J., Eds.; Kluwer Academic Publishers: Dordrecht, The Netherlands, 2000; p 499.

(2) Michl, J. *Acc. Chem. Res.* **1990**, *23*, 127.

(3) Miller, R. D.; Hofer, D.; Rabolt, J. F.; Fickes, G. N. *J. Am. Chem. Soc.* **1985**, *107*, 2172. Harrah, L. H.; Zeigler, J. M. *J. Polym. Sci., Polym. Lett. Ed.* **1985**, *23*, 209. Yuan, C.-H.; West, R. *Macromolecules* **1998**, *31*, 1087.

(4) Schilling, F. C.; Bovey, F. A.; Davis, D. D.; Lovinger, A. J.; MacGregor, R. B., Jr.; Walsh, C. A.; Zeigler, J. M. *Macromolecules* **1989**, *22*, 4645. Song, K.; Kuzmany, H.; Wallraff, G. M.; Miller, R. D.; Rabolt, J. F. *Macromolecules* **1990**, *23*, 3870. Song, K.; Miller, R. D.; Wallraff, G. M.; Rabolt, J. F. *Macromolecules* **1991**, *24*, 4084.

(5) Miller, R. D.; Sooriyakumaran, R. *Macromolecules* **1988**, *21*, 3120. Oka, K.; Fujiue, N.; Dohmaru, T.; Yuan, C. H.; West, R. *J. Am. Chem. Soc.* **1997**, *119*, 4074.

(6) Neumann, F.; Teramae, H.; Downing, J. W.; Michl, J. *J. Am. Chem. Soc.* **1998**, *120*, 573.

(7) Michl, J.; West, R. *Acc. Chem. Res.* **2000**, *33*, 821.

(8) Teramae, H.; Michl, J. *Mol. Cryst. Liq. Cryst.* **1994**, *256*, 149.

(9) Albinsson, B.; Teramae, H.; Downing, J. W.; Michl, J. *Chem. Eur. J.* **1996**, *2*, 529.

(10) Albinsson, B.; Antic, D.; Neumann, F.; Michl, J. *J. Phys. Chem. A* **1999**, *103*, 2184.

(11) Ottosson, C. H.; Michl, J. *J. Phys. Chem. A* **2000**, *104*, 3367.

(12) Fogarty, H. A.; Ottosson, C. H.; Michl, J. *THEOCHEM* **2000**, *506*, 243.

(13) Fogarty, H. A.; Ottosson, C. H.; Michl, J. *J. Mol. Struct.* **2000**, *556*, 105.

(14) Belyakov, A. V.; Haaland, A.; Shorokhov, D. J.; West, R. *J. Organomet. Chem.* **2000**, *597*, 87.

(15) Shafiee, F.; Haller, K. J.; West, R. *J. Am. Chem. Soc.* **1986**, *108*, 5478. Sekiguchi, A.; Nanjo, M.; Kabuto, C.; Sakurai, H. *J. Am. Chem. Soc.* **1995**, *117*, 4196. Suzuki, H.; Kimata, Y.; Satoh, S.; Kuriyama, A. *Chem. Lett.* **1995**, 293. Lambert, J. B.; Pflug, J. L.; Denari, J. M. *Organometallics* **1996**, *15*, 615. Lambert, J. B.; Pflug, J. L.; Allgeier, A. M.; Campbell, D. J.; Higgins, T. B.; Singewald, E. T.; Stern, C. L. *Acta Crystallogr. C* **1995**, *51*, 713.

(16) Zink, R.; Magnera, T. F.; Michl, J. *J. Phys. Chem. A* **2000**, *104*, 3829.

(17) Albinsson, B.; Michl, J. *J. Phys. Chem.* **1996**, *100*, 3418.

(18) Imhof, R.; Teramae, H.; Michl, J. *Chem. Phys. Lett.* **1997**, *270*, 500.

(19) Tsuji, H.; Toshimitsu, A.; Tamao, K.; Michl, J. *J. Phys. Chem. A* **2001**, *105*, 10246.

(20) Albinsson, B.; Teramae, H.; Plitt, H. S.; Goss, L. M.; Schmidbaur, H.; Michl, J. *J. Phys. Chem.* **1996**, *100*, 8681.

(21) Crespo, R.; Teramae, H.; Antic, D.; Michl, J. *Chem. Phys.* **1999**, *244*, 203.

(22) Crespo, R.; Merchán, M.; Michl, J. *J. Phys. Chem. A* **2000**, *104*, 8593.

(23) Piqueras, M. C.; Merchán, M.; Crespo, R.; Michl, J. *J. Phys. Chem. A* **2002**, *106*, 9868.

(24) Frisch, M. J.; et al. *Gaussian 98*, Revision A.7; Gaussian Inc.: Pittsburgh, PA, 1998.

(25) Kendall, R. A.; Dunning, T. H., Jr.; Harrison, R. J. *J. Chem. Phys.* **1992**, *96*, 6796.

(26) Scott, A. P.; Radom, L. *J. Phys. Chem.* **1996**, *100*, 16502.

(27) Widmark, P. O.; Persson, B. J.; Roos, B. O. *Theor. Chem. Acta* **1991**, *79*, 419.

(28) Piqueras, M. C.; Crespo, R.; Michl, J. *Mol. Phys.* **2002**, *100*, 747.

(29) Andersson, K.; Malmqvist, P. A.; Roos, B. O. *J. Chem. Phys.* **1992**, *96*, 1218.

(30) Roos, B. O.; Taylor, P. R.; Siegbahn, P. E. M. *Chem. Phys.* **1980**, *48*, 157.

(31) Finley, J.; Malmqvist, P. A.; Roos, B. O.; Serrano-Andrés, L. *Chem. Phys. Lett.* **1998**, *288*, 299.

(32) Forsberg, N.; Malmqvist, P.-Å. *Chem. Phys. Lett.* **1997**, *274*, 196.

(33) Malmqvist, P. A.; Roos, B. O. *Chem. Phys. Lett.* **1989**, *155*, 189.

(34) Andersson, K.; et al. *Molcas 5*; Department of Theoretical Chemistry, University of Lund: Lund, Sweden, 2001.

(35) Bock, H.; Ensslin, W. *Angew. Chem., Int. Ed.* **1971**, *10*, 404.

(36) Imhof, R.; Antic, D.; David, D. E.; Michl, J. *J. Phys. Chem. A* **1997**, *101*, 4579.

(37) Tsuji, H.; Imhof, R.; Fogarty, H. A.; Downing, J. W.; Ehara, M.; Nakatsuji, H.; Tamao, K.; Michl, J. Unpublished results.

(38) Ernst, C. A.; Allred, A. L.; Ratner, M. A. *J. Organomet. Chem.* **1979**, *178*, 119.

(39) Fogarty, H. A.; David, D. E.; Ottosson, C.-H.; Michl, J.; Tsuji, H.; Tamao, K.; Ehara, M.; Nakatsuji, H. *J. Phys. Chem. A* **2002**, *106*, 2369.

(40) Plitt, H. S.; Michl, J. *Chem. Phys. Lett.* **1992**, *198*, 400.

(41) Plitt, H. S.; Downing, J. W.; Raymond, M. K.; Balaji, V.; Michl, J. *J. Chem. Soc., Faraday Trans.* **1994**, *90*, 1653.